Radar based human vital sign detection in cars

Signal processing

Group 3

July 7, 2020

Achinuhu, Ikenna
Hsiao, Xian Cheng

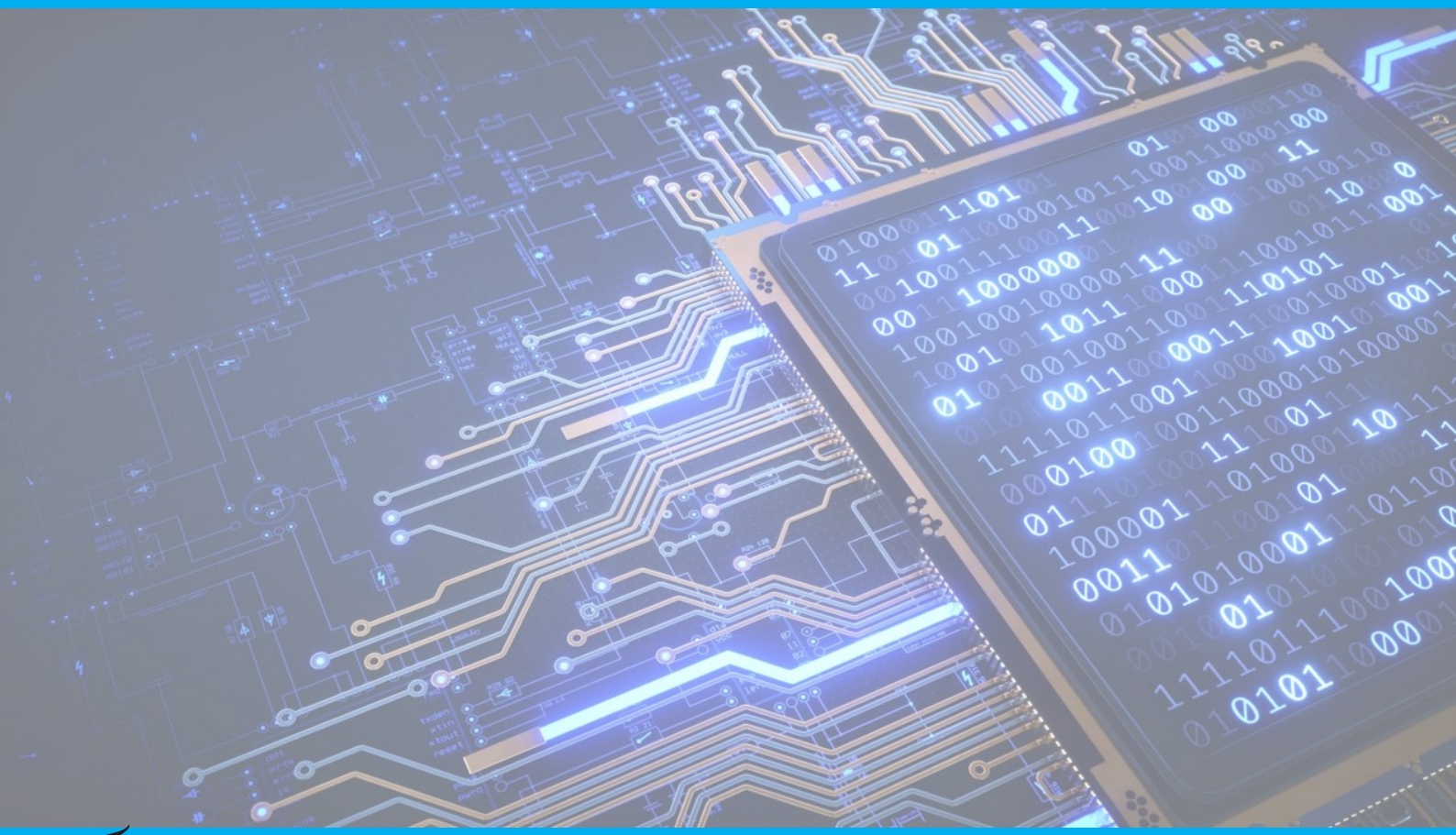

TU Delft

Bap Thesis 2020

Group 3: Signal Processing

Achinuhu, Ikenna, 4722507
Hsiao, Xian Cheng, 4653947

July 7, 2020
Delft

Delft University of Technology
Faculty of Electrical Engineering, Mathematics and Computer Science
Electrical Engineering Programme

Contents

1

Abstract

In this thesis signal processing techniques for the Ultra wide-band impulse radar (UWB-IR) radar are discussed. To context wherein these algorithms are used is in a car, with the aim of detecting a child left behind in the car. This thesis also touches on algorithms to obtain vital information of the child inside the car. To this end a mathematical model for chest movement causes by breathing and heart beat is made and explained. From this mathematical description data is derived in the form of a range-time matrix in MATLAB.

The functioning of the algorithms are then showcased using this data. Regarding the algorithms. This thesis discusses 3 potential filters that can be implemented in the signal processing scheme. These are the adaptive, average and exponential filters. Their hardware implementation is spoken of as well as their implementation in MATLAB.

The algorithm for detecting of humans are also covered with emphasis on the threshold used for this. Finally the last step in the signal processing scheme, the measuring of breathing- and heart-beat frequency , is worked out in the form of four additional algorithms which include:

- Fast fourier transform
- Hilbert huang transform
- The centroid algorithm
- cumulative summation

This thesis then finally tests these four algorithms in form of a complete signal processing algorithm (filter+human detection+vital sign detection) using real world experimental data. Then by considering all aspects of the scheme, from hardware implementation, efficiency, functionality and precision, the algorithm that works best for our goal of detecting a child in a car is chosen.

2

Preface

The goal of this project is to create a radar system that's capable of detecting babies being left inside a car. This particular thesis is about the the signal processing after the radar, about how to best process information gained by the radar, so that it can achieve the aforementioned goal.

Thus in this thesis an overview of the different signal processing techniques will be given and the effectiveness of these techniques will be showcased using our synthetic data as well as experimental data obtained from an uwb-ir radar, along with a comparison of the efficiency and the complexity of these techniques will be made. It needs to be noted that this thesis was written during the COVID-19 pandemic and thus most of the measurement data used in the thesis was measured by another university under unknown circumstances. This however does mean that the data used isn't the same as the data we would have measured given the opportunity to measure our own data.

3

Introduction

3.1. Introduction

Radar is a widely used technology, whether its used to locate or extract information from certain objects, radar technology sees its use in many fields [1]. One of those fields being the detection of human beings and/or extraction of vital signs, which is the basis of our graduation project. Every year an average of 38 kids in the US lose their lives inside a cars as a result of the heat [2]. Even just last year in 2019, 15 kids died as a result of being forgotten inside of a hot car by their parents, the so called heatstroke-deaths. With this graduation project, the aim is to develop a detection system that can prevent this and is fully implementable inside a car. Radar is extremely well suited for this purpose.

While there are many different types of radar, they all work according to the same principle [3]. In a radar the transmit antenna sends out an electromagnetic wave whose reflections, created by collisions of the wave with objects, gets picked up by the receive antenna. By then comparing the received wave with initial one, information about the space that the radar is inside of can be obtained. When the aforementioned object is a person it becomes possible to not only know if the person is present (or the child is still inside the car), but it can also be taken one step further to the point of measuring the person's breathing or even heartbeat. For the graduation project our sub-group mainly focuses on the signal processing aspect of the radar implementation (see figure 3.1). This means that in this thesis the part that actually translates the information received by the radar into something that is useful is created and worked out.

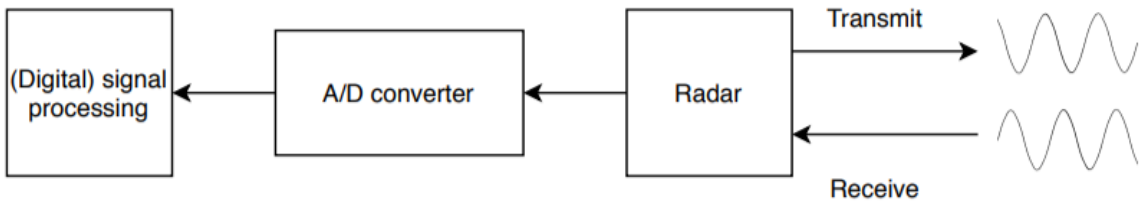

Figure 3.1: Basic building blocks of a radar

3.2. State of the art analysis

As mentioned there are many types of radars that are capable of extracting the vital signs of a person. Most of these radars fall under the guise of Doppler radar [4]. Many of these radars are already seeing their use in the medical field. The paper "Human Vital Signs Detection Methods and Potential Using Radars: A Review" [5]. showcases a lot of these different radar types, their possibilities when it comes to signal processing and their uses in the medical field.

3.2.1. Continuous wave radar

The most commonly used radar types are the continuous wave (CW) [[6], [7]] (both frequency modulated FMCW ([8], and stepped frequency continuous wave (SFCW)). The continuous wave radar sends out a continuous wave (hence the name), whose frequency upon being reflected by a moving target, such as a person's chest during breathing, changes in frequency. The paper by [6] gives the following mathematical description of the received CW-radar wave:

$$R(t) = A_R * cos\big(2 * \pi * f - \frac{4\pi * d_0}{\lambda} - \frac{4\pi * x(t)}{\lambda} + \theta(t - \frac{2d_0}{c})\big) \tag{3.1}$$

"where A_R, f and λ are the amplitude, the frequency and the wavelength of the carrier sine wave signal, c is the speed of light, d_0 is the nominal radar-target distance and x(t) is the displacement due to breathing and heartbeat" [6]. This description is also similar to that used in the paper of [7]. It shows that the chest displacement modulates the carrier signals frequency. This technique however has a few downsides such as: the null-point problem, penetration of materials. Which were mentioned in the paper of [9]. CW are also subject to motion artifacts which can be removed using an IIR filter [7].The paper [5] also mentions these shortcomings in addition to phase noise created by the local oscillator as well as problems regarding signal corruption origination from random body movement (RBM) and difficulties regarding separations of the heartbeat and respiration signals as well as when multiple target detection. The paper however also makes mention of the fact that the phase noise and the null-point detection could be solved using (sophisticated) signal processing techniques.

The so called microwave Doppler radio[[10]] are an older implementation of the continuous wave, but follow the same principle.

3.2.2. Ultra wide-band radar

Another more recently used radar technique is the ultra wide-band radar (UWB) [11], [12], [9] which instead of sending a continuous wave form, sends a single pulse every time instance. The impulse radio ultra wide-band radar (IR-UWB) is the most commonly used [5]. There are also a few other types of UWB radars where for example the pulses are modulated with a frequency [3]. The basic workings of the UWB are illustrated by figure 3.2.A and 3.2.B. The radar sends out a pulse every time instance and also receives this pulse for a certain duration. Now since the distance between the antenna and the person reflecting the initially sent pulse is periodically changing, the time it takes for the pulse to arrive also differs from time instance to time instance. Causing small delays in the received signal. Drawing a line straight down through all the sent pulse (like in figure 3.2.B) and looking at how the signal differs, makes it possible to extract the frequency information that caused these differences.

Human vital signs when it comes to breathing only happen in a certain range:

- a) breathing with a frequency band between 0.2 and 0.5 Hz and the thorax and chest movement amplitude of 0.5–1.5 cm; [12]
- b) heartbeat with a frequency band between 0.8 and 2.5 Hz and the chest motion amplitude of 2–3 mm; [12]

3.3. Problem definition

In the world, numerous babies and pets die as a result of being left behind in a car. In 2018, as much as 52 children have died in the U.S., because they were forgotten and trapped in a car [13]. With the rising temperature caused by global warming, the numbers of death around the world in the future will only be higher. These deaths must be prevented under all circumstances. These deaths are not only happening in the U.S., but in the whole world, no matter in what part of the world this is. To prevent this, the radar system will be able to give the user a signal telling that the user forgot his or her baby in the car.

This radar system will be working whenever the car is powered on and determines the breathing of the baby. When the car is powered off the radar system will switch to its internal power supply and notify the user about the baby left inside the car. At this point the user will remember to take the baby along with him or her and a death by heatstroke is prevented.

3.3.1. SMART

Using SMART technique, it is possible to analyse the goals being set up, the feasibility and also determine the possible constraints.

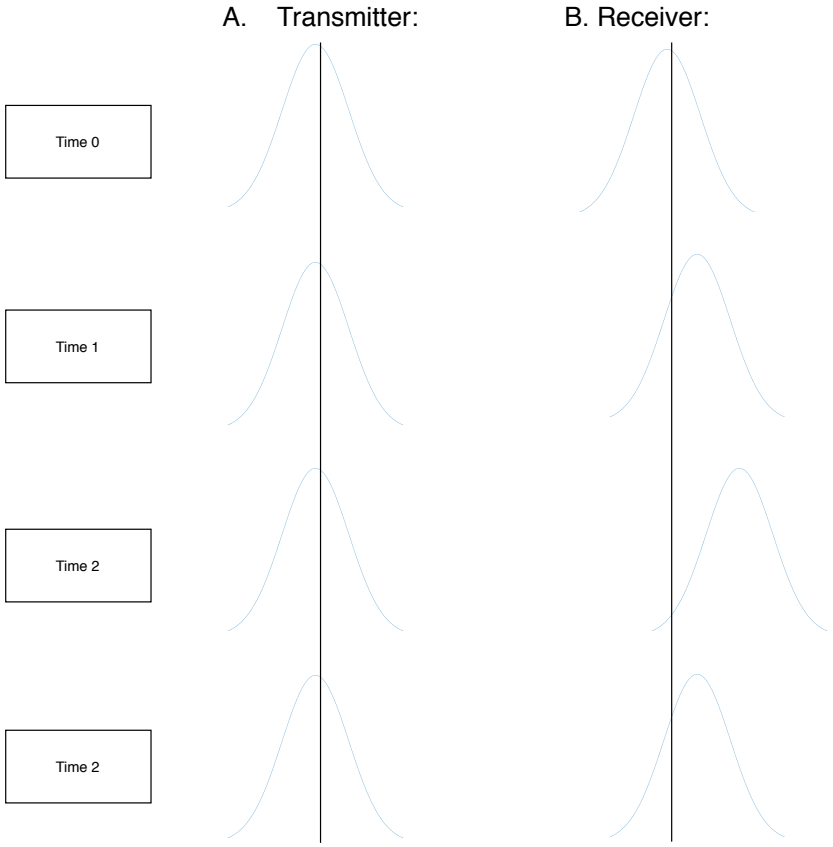

Figure 3.2: Pulses sent and received by UWB transmitter

- Specific: Detection of baby left inside a car to prevent death by heatstroke.
- Measurable: The presence of the baby inside a car.
- Achievable: Remind the user that a baby is left inside a car.
- Realistic: Decrease the change of a baby left in a car having a heatstroke.
- Timely: The user should be notified within 5 minutes.

For the radar system it is important use as little power as possible to prevent any concerns about the safety of the baby caused by the radar system, this power should comply with the safety standards of FCC [[14]]. The radar should also be fully operational under the temperature fluctuations of day and night in the west and the east of the world, while easy to implement inside a variety of cars.

3.4. Contribution of the thesis

This study will determine an algorithm that is well suited for a dynamic placing of the radar to comply with the different objects in a vehicle. In this report we have used synthetic data generated using MATLAB, which resembles the data acquired from a UWB-IR radar, and experimental data obtained from a XeThru UWB-IR radar to approach the desired goals. The data from the XeThru radar is acquired by third party institutions and does not include the environment or the setting in which the experiment took place. The data will include a human breathing with a specific heart rate that is translated into a range time matrix. Using the data, the algorithm, deployed in three parts, will determine the distance of the human as well as the extraction of the breathing rate and the heart rate.

4

Programme of Requirements

To address the requirements, it is important to focus on the environment in which the radar system is operating, inside a vehicle. In this context, the radar system ought not to interfere with the performance of the car, nor with the actions of what someone does inside a car such as blocking the sight or movement ,or draw too much power. As the radar system will be implemented to detect babies left inside a car, the system needs to be able to function in a variety of different vehicles with different objects around the target. To have the radar work during its most critical operating window, shortly after the car has been turned off, the system should have an extra power supply to adjust to the loss of the power from the car for at least 30 minutes, this can be done via a small battery cell.

There are other requirements which focuses on the human which the radar system is targeting, the safety of a baby or a pet. To ensure the safety of the baby, the power of the radar should not exceed a Specific Absorption Rate (SAR) of 4W/kg [15] at frequencies lower than 6Ghz. This limit will likely be too high for the frequencies that the XeThru is operating in (7.4Ghz), the limit would be lower for higher frequencies.

For the algorithm it is important to have them compute in real time, and as simple as possible. As the algorithm gets simpler, less hardware will be needed and power consumption will also decrease.

4.1. Specific system requirements

- Able to detect babies inside a car
- Internal power supply (Cell battery)
- Compliant with safety standards (<2W/kg) (FCC, European Union, ICNIRP)
- Small form factor (XeThru size)
- Easy to implement inside a car
- Can be implemented in most cars

4.1.1. Optional system requirements

- Pet detection inside a car
- Breathing rate detection
- Heart rate (frequency bandwidth from 0.8 to 2.5 Hz)
- rate within 0.01 Hz of actual value (resolution 0.01 Hz)
- Low complexity
- Baby detection for all possible models of baby-seats

4.1.2. Algorithm requirements

- Real-time calculations (Algorithm based on data stream)
- Breathing rate detection (frequency bandwidth from 0.2 to 0.5 Hz)
- Heart rate (frequency bandwidth from 0.8 to 2.5 Hz)
- Breathing/Heart rate within 0.01 Hz of actual value (resolution 0.01 Hz)
- Data simplification
- Computational light
- Environment independent
- Low power consumption (<300mW)

Using a typical coin cell bettery CR2032, figure 4.1, the power in the cell is 220mAh at 3V, which is 660mWh. To use this battery as a backup power for when the car is turned off, it should last 30 minutes, which is 1200mW. To account for battery degradation and possible power leakage, the maximum power consumption is at 300mW. The battery will be charged every time the power supply is up again to ensure power is always availible.

Figure 4.1: Coin cell battery CR 2032. Source: Wikipedia

The algorithm also needs to simplify the data from the radar, the data stream can best be simplified to a various number related to the distance. This will help with the total amount of computation needed.

5

Signal processing schemes

5.1. Data

In order to confirm the effectiveness of the algorithms created in this project, they need to be tested on actual data, to see if it is possible to actually detect humans or measure the vital signs. In this project two types of data are used: experimental data measured by another university and synthetic data that was created ourselves and with which it is possible to change certain parameters on the spot to see how the algorithms react. Thus the synthetic data will be used to showcase the effectiveness of the data, after which the experimental data is then used to see how the algorithms react on a real world example, data which includes noise, multipath reflections etc. Since this project is based on the UWB-IR radar, the data received by the radar comes in the form of a range-time-intensity (RTI) matrix. In this matrix each row contains the pulse received. The different columns or the x axis is called fast-time and the unit is metres. The different rows or y axis is called the slow time are the moments when the radar start receiving a new set of values from the electromagnetic wave.

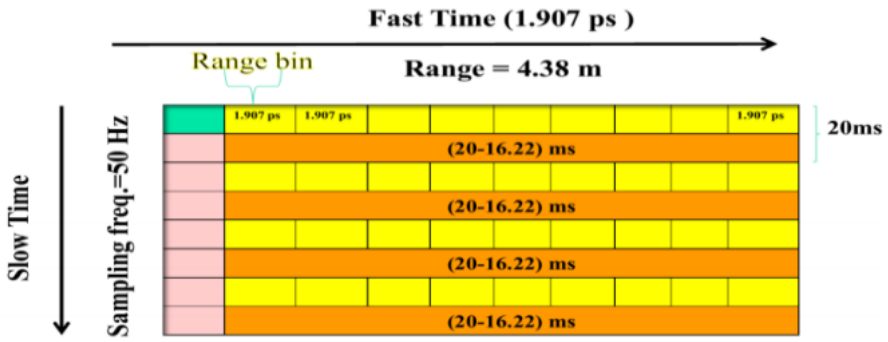

Figure 5.1: example of range(fast time) time(slow time) data collection diagram.
[16]

5.1.1. Mathematical interpretation

To create synthetic data that can be interpreted as radar pulses reflected of a moving chest, it is important to have a good mathematical description to act as a model. Many different paper and articles have set out to do this very thing [[17] [9] [16]]. Most literature agrees that the best way to model the chest displacement, caused by breathing and heart rate, is as two sine waves. [16] models breathing as:

$$d(t) = d_0 + \sum_{i}^{M} c_i * sin(2\pi * i * f_b * t) + \sum_{j}^{N} a_j * sin(2\pi * j * f_b * t) \tag{5.1}$$

Where d0 is the distance from the person to the radar. $c_i and a_j$ are the harmonic components of chest and abdomen displacement with M and N the highest harmonic component. This however might not be the best model as it increases the complexity by considering both abdomen and chest displacement and ignores the displacement caused by the heart beat. Also when it comes to data used for testing algorithms, the higher harmonics can be ignored since they would simply clutter the results, and also when it comes to vital detection, these higher harmonics would be removed either way before applying the vital detection algorithms. A better more simpler model would be:

$$d(t) = d_0 + m_b * sin(2\pi * f_b * t) + m_h * sin(2\pi * f_h * t) \tag{5.2}$$

Where $m_b and m_h$ are chest displacement amplitude caused by breathing and heart beats. Since electromagnetic waves travel with the speed of light, the time it takes for the wave to be received would be:

$$\tau_d(t) = 2 * d(t)/c = d_0/c + \frac{m_b}{c} sin(2\pi * f_b * t) + \frac{m_h}{c} sin(2\pi * f_h * t) \tag{5.3}$$

The model for the received signal then becomes:

$$r(t,\tau) = \sum_i A_i * p(\tau - \tau_i) + A * p(\tau - \tau_d(t)) \tag{5.4}$$

where p(t) is the normalized received pulse, A_i is the amplitude of each multi-path component,τ_i the delay of the i-th static multi-path, and A is the amplitude of the pulse reflected on the body. So the summation are the effects of the environment which when concerning the synthetic test data can be ignored. The term on the right denotes the actually pulse which delay is modulated by the person's chest. The received signal will be measured in discrete time intervals in slow time $t = n * T_s n = 1,2,3,...,N$. which results in N pulse sequences (rows) which each are also sampled with $t = m * T_f m = 1,2,3,...,M$ (fast time) which results in M rows.

The pulses sent by the radar can be approximated by using a gaussian waveform [[18]]. The paper "Ultra-wideband impulse radar-an overview of the principles" by [18] gives as the following equation as mathematical description:

$$\Omega(t) = A * e^{-4\pi(\frac{t}{\Delta T})^2} \tag{5.5}$$

Where ΔT would be the bandwidth of the pulse and $1/(\Delta T)$ the bandwidth of the pulse in frequency domain.

5.1.2. Synthetic data

To create our synthetic data, the mathematical model is used, where $d_0 = 1m$, m_b is around $4-12mm$ and at f_b around $0.2-0.34Hz$, with the chest movement due to the heart beating, m_h is around $0.2-0.5mm$ at f_h around $1-1.34Hz$ [[19]. We have chosen to model the chest expansion with $m_b = 8mm$ at $f_b = 0.25Hz$, $m_h = 0.5mm$, and $f_h = 1.2Hz$.

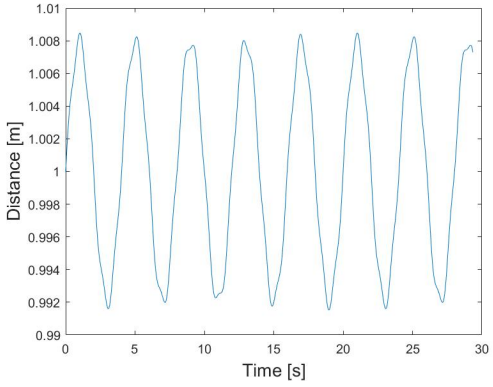

(a) Synthetic Time-Distance graph with a breathing rate and heart rate of $m_b = 0.008m$, $f_b = 0.25Hz$, $m_h = 0.0005m$, $f_h = 1.2Hz$ at a distance of $d_0 = 1m$

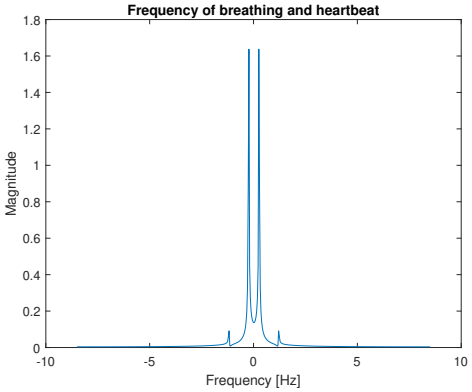

(b) Fourier transform of the synthetic distance at $D_0 = 0$ with a peak at 0.25Hz and 1.2Hz.

Figure 5.2: Time domain waveform and frequency spectrum of the synthetic distance

The pulse repetition frequency is used to be above the Nyquist frequency of the breathing rate which needs to be at least 2x the heart rate, 2x higher than 1.2Hz. We have chosen to have 14x the Nyquist frequency as our PRF at 17Hz, which is the same as our experimental data. Since the target is at 1 meter, we only need to have the details around 1m, with a large enough range to detect the various distances.

Variable	Value
m_b	8 mm
f_b	0.25 Hz
m_h	0.5 mm
f_h	1.2 Hz
PRF	17 Hz
$Range$	200 mm
$RangeBins$	50
$Duration$	30 s
$NumFrames$	500

Table 5.1: Configurations for the synthetic data

These parameters are the ones that closely emulate real life breathing as far as the model goes, since for breathing the frequency lies between 0.2 and 0.5 Hz with a maximum amplitude of 1.5 cm and for heart beat this is 0.8-2.5 mm with an amplitude of 3 mm as maximum. In this thesis however, a few graphs may be plotted using slightly more unrealistic parameters in order to make the explained graphs and concepts more clear.

For the implementation of the mathematical model in MATLAB a function called chest_model was written. The function takes the parameters mentioned earlier in as arguments, and calculates the total distance from radar to person and total time it would take for a electromagnetic wave to travel that distance for a given time (slow-time). It's also possible to give the function a vector of different time values in which case it would return a vector with different values for the distance or time delay. Plotting this, results in figure 5.2a. The code for the function can be found in appendix A.2.

To illustrate that the chest model works, the frequency spectrum is calculated using the fft on the distance vector and plotted. For this test the frequencies of the sines were set to 0.5 and 1.5 Hz and the amplitudes to 5 mm and 2 mm. The code for the testing can be found in the appendix.

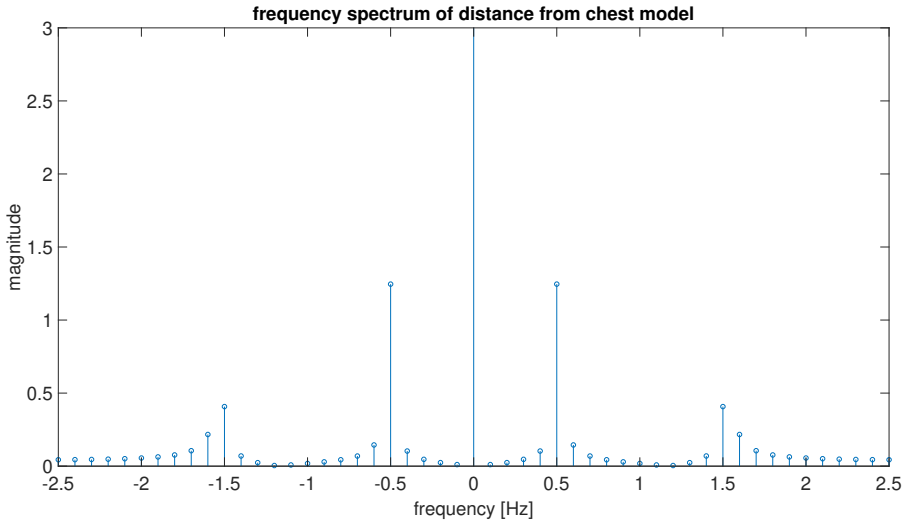

Figure 5.3: Spectrum of distance vector from chest model with $m_b = 0.05m$, $f_b = 0.5Hz$, $m_h = 0.05m$, $f_h = 1.5Hz$ at a distance of $d_0 = 2m$

As was already expected 5 peaks can be seen. One at DC and 4 at +/-0.5Hz and +/-1.5Hz.

Now for the synthetic data to emulate the UWB-IR radar, pulses are created where every pulse is delayed with the amount given by the distance vector. So the pulse send at slow time x will be delayed with a range of distance[x]. This can be visualised in figure 5.4 by using the Gaussian distribution on the distance vector in

figure 5.2a with the variables in table 5.1 and the variance $\sigma = 4/1.5e3$, this variance is chosen large enough to comply with our "sampling rate". The actual sampling rate of the XeThru radar, at 23.328GHz, will be able to detect the actual width of the pulse $t = 1/1.5 \cdot 10^9 s$, and down-sampled to base-band signal.

The pulses are created by the $normpdf$ function with the shape of a Gaussian distribution and the peak of the pulse set to the distance from radar to the target. So the first pulse has a peak at d0 and the pulse after that has a peak slightly to the right. To illustrate this 20 of these pulses are plotted in the figure 5.4 with a slightly bigger pulse width. Plotting the RTI matrix for the synthetic data results in:

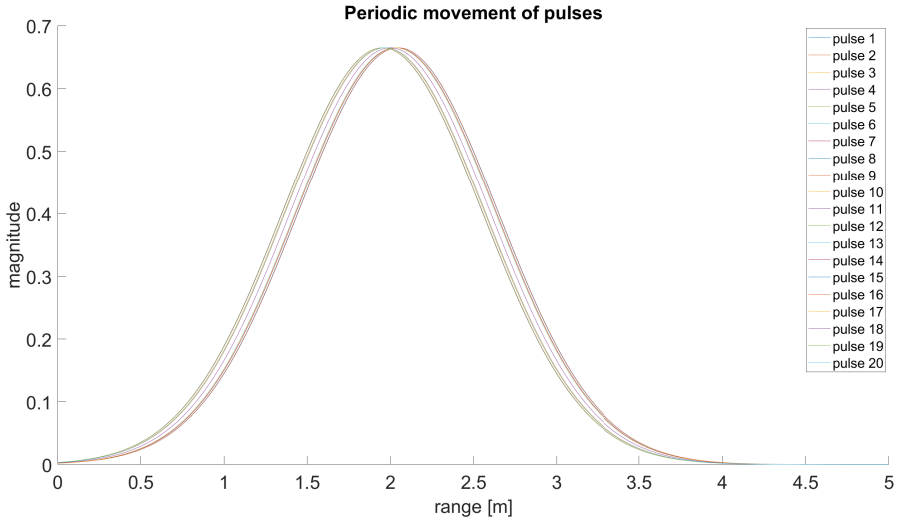

Figure 5.4: 20 Pulses with their peaks periodically moving around 2m

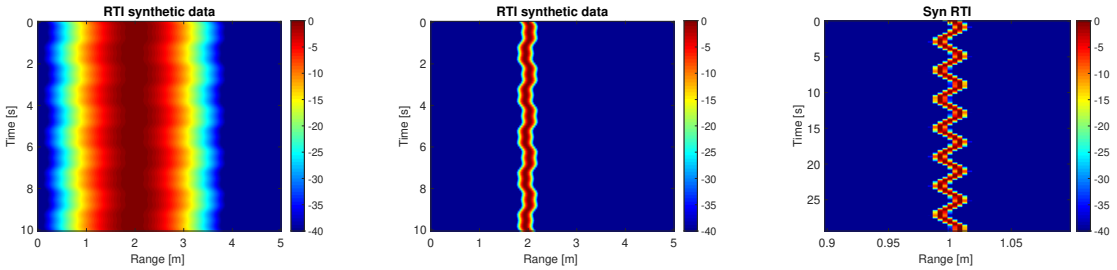

(a) RTI matrix of synthetic data fb=0.5 and fh=1.5 with normpdf standard deviation set to 0.6

(b) RTI matrix of synthetic data fb=0.5 and fh=1.5 with normpdf standard deviation set to 0.06

(c) RTI matrix of synthetic data using values from table 5.1

Figure 5.5: RTI matrix of synthetic data with different parameters

5.1.3. Experimental data

As mentioned in the preface, the experimental data used to test the created signal processing algorithms where made by students of another university. So, while it is clear that the data is indeed that of a uwb radar measuring the movements of someone's chest, there is no way to know how the experiment was exactly set-up. With more emphasis on the environment and location the researchers were in during the measuring of the data. There is however a lot of different measurements available. Two different people were measured, with each sitting at different distances from the radar (1m, 2m, 3m, 4m and 5m). Data of an empty room was also available as well as some data with the subject sitting at a different angle from the radar and not directly towards it.

5.2. Three-part algorithm

5.2.1. General design

To identify the target's distance from the radar, a moving target indicator (MTI) is used to suppress the static targets and enhance the movement of the baby. The signal then passes a first order low-pass filter to reduce the noise captured by the radar. This final signal will be used to determine the baby and perhaps also its breathing rate and heart rate. As our algorithm needs to do a variety of tasks, it is best to also split the algorithm into three parts, MTI and low-pass filter, Human detection, and breathing and heart rate estimation.

1. MTI and Low-pass filter
2. Human detection
3. Vitals detection

The first part, which is the filter, deals with the unprocessed signals and eliminates the static clutters. This ensures that the data is not affected by other objects, and the human baby is more visible. The low-pass filter ensures that the majority of the higher frequency noise is removed. The second part is to detect the presence of the baby, and to determine the distance of the baby with respect to the radar. Here it is also possible that a pet is detected instead of a baby. The last part of the algorithm detects the breathing rate and also the heartbeat of the baby, this algorithm focuses on the signal with the baby.

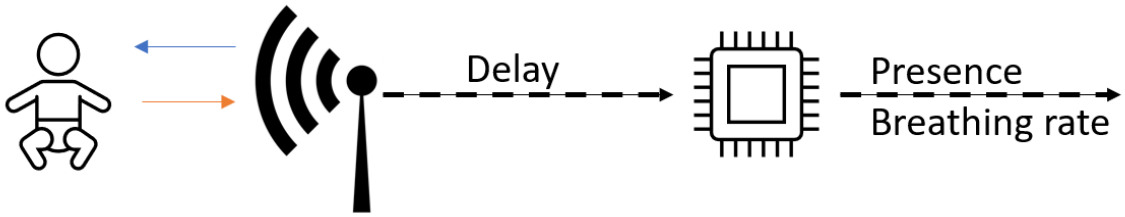

Figure 5.6: Basic principle of the radar system from the baby to the final output

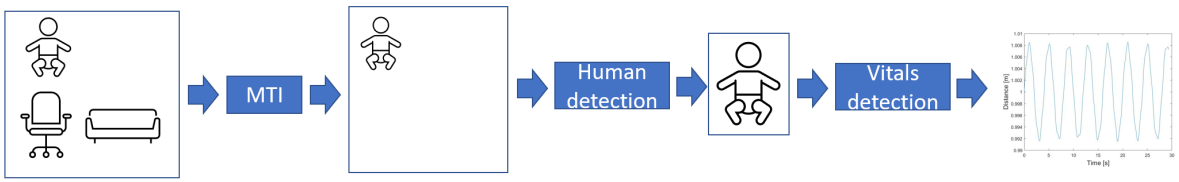

Figure 5.7: Basic principles of the algorithms used from distinguishing the baby to its breathing rate

6

Processing

Before the detection of vital signs can be done on the data, the data itself needs to be processed in such a way that the algorithms for the vital sign detection are able to work as efficient and accurate as possible. So in this chapter the pre-processing algorithms used on the data before the vital sign detection are worked out and explained. These include filtering the signal, detecting the presence of a person and finally an algorithm to facilitate specific frequency detection methods such as the fast Fourier transform.

6.1. MTI and Filter

In an ideal case we want the baby in free space to have a fully reflective chest that can reflect everything, this means that the reflected signal is intense and clear at the point of the chest and has no multi-path signals. In reality, the signal is blurred and has a lot of static objects interfering with the reflected signal from the baby. These signals needs to be filtered out in order to determine the distance of the baby as seen in figure 6.1.

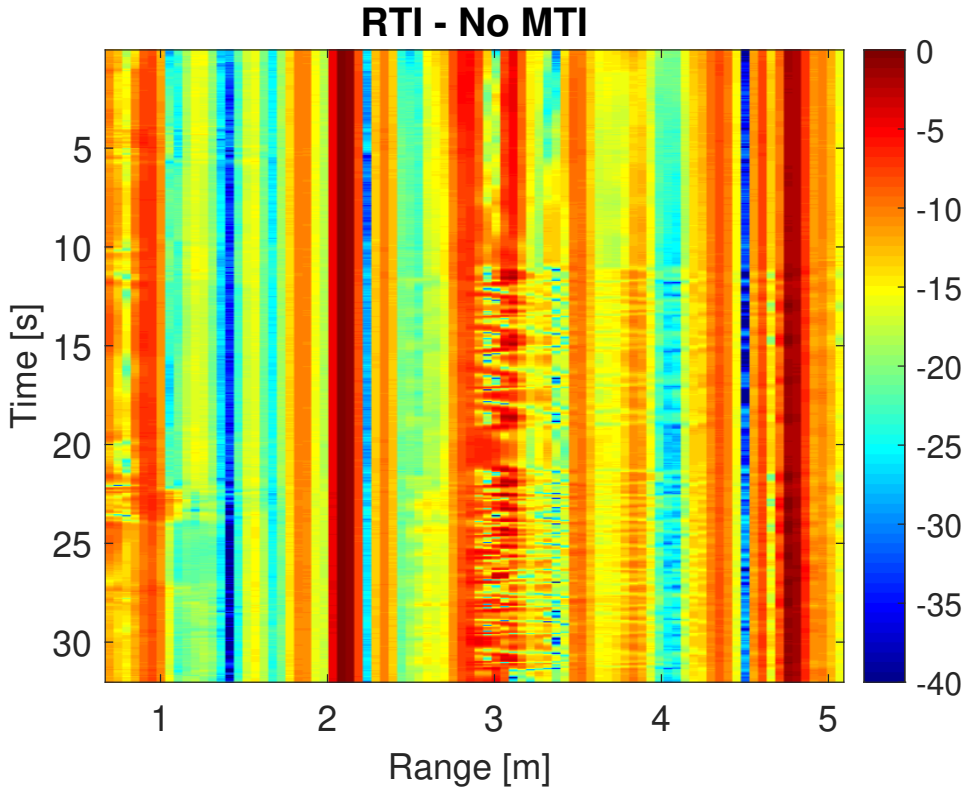

Figure 6.1: Experimental signal-Reflected signal with no filter for a human at 3m distance.

In figure 6.1 the reflected signal from the human is not visible at the first sight, this is because the signal is distorted by the reflections of the static objects. At 3 meters the signal is distorted, meaning that the reflected signal is coming, in this case, from a human. To eliminate the static objects a filter is used, and different algorithms are compared. These algorithms are:

- Average filter
- Adaptive filter
- Exponential filter or moving average filter

These algorithms will be compared in a performance factor, hardware requirements and speed.

6.1.1. Average filter

The average filter, figure 6.2, uses the average of the signal in time axis, in our simulation the time is 30 seconds, and assumes that the average signal are the static reflections. These static reflections will be subtracted from the radar profile, and the remaining data should be that of a human, multi-path signal or anything that moves. To make the average filter there needs to be more registers to store the data that needs to be recorded which requires extra hardware. This algorithm also needs some time to record and calculate the average before the signal can be processed, after which the calculation is a simple subtraction which is done in real time.

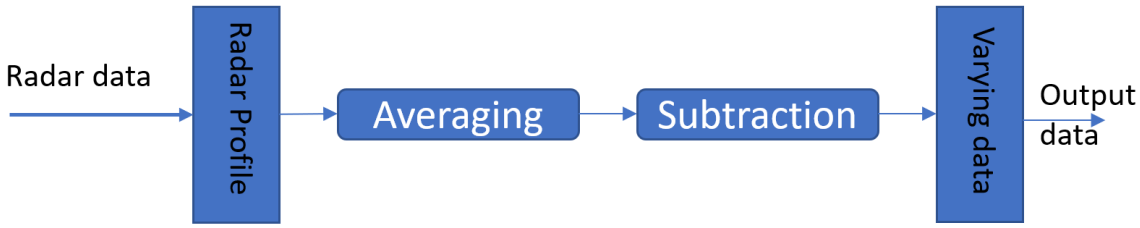

Figure 6.2: Block diagram of an average MTI filter

6.1.2. Adaptive filter

The adaptive filter, figure 6.3, will adapt to the signal and remove the static clutters that is present in the data. Here we subtract from each radar profile the previous profile weighted by 95% and the current profile weighted by 5%. This algorithm will need to use multiple registers at the same time to store the previous data and also to hold the current data as well as the data that is calculated. Overall, the complexity of this algorithm will be higher than the average filter, but is still a simple implementation.

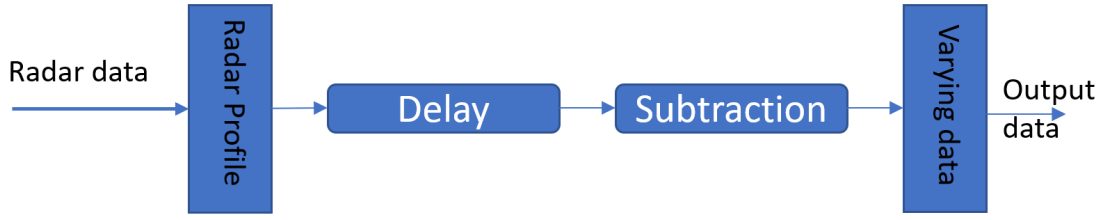

Figure 6.3: Block diagram of an adaptive MTI filter

6.1.3. Exponential filter

The exponential filter, or a moving average, figure 6.4, will use a recursive calculation in which 30% of the new radar profile will be added to 70% of the old moving average. This creates a exponential pattern where the older data gets depreciated as the data gets outdated, and the moving average will adapt to the newer data sets. To implement this in hardware the moving average acts like a first order system which is simple to implement and not too complex.

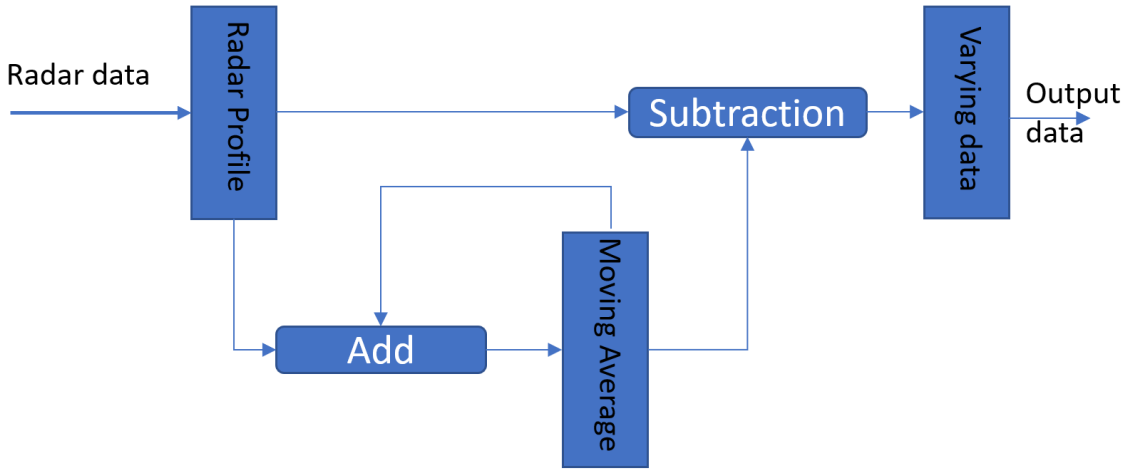

Figure 6.4: Block diagram of an exponential MTI filter

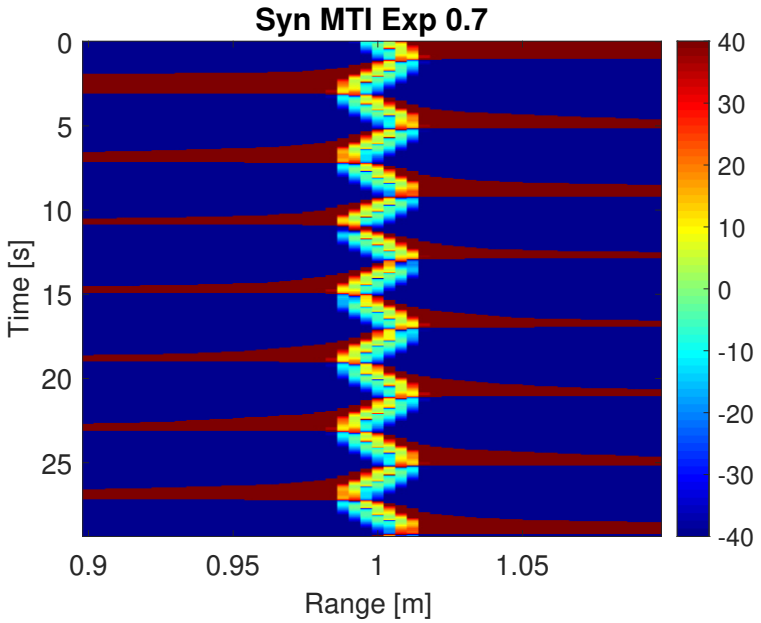

Figure 6.5: Signal after the exponential filter with a signed dB magnitude

In figure 6.5 the outputs of the exponential MTI filter is shown with a signed dB magnitude, meaning that the magnitude of the difference signal is in dB and then the original sign is added for a positive and negative visualisation. In this setup, increasing by a little would mean that in the graph the signal would be very high, whereas the part with the most fluctuations is around 0 dB.

As the three MTI filters are relatively simple to implement, the performance is crucial to the final decision. A performance factor will be calculated using the signal strength of the person and divide it by the noise

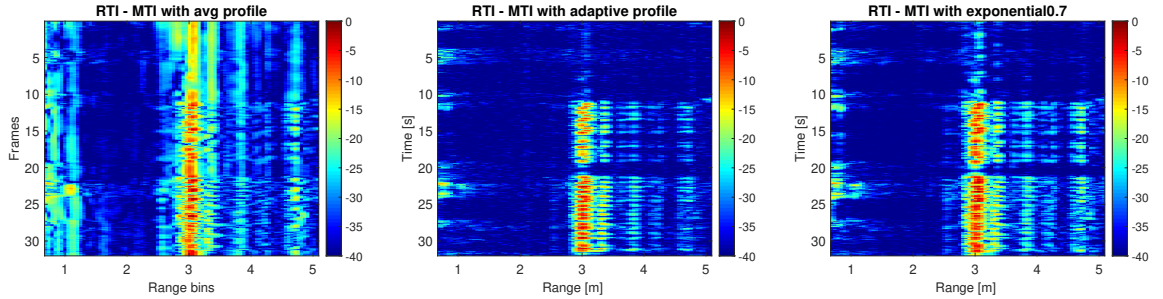

(a) Reflected signal using average filter at 3m distance

(b) Reflected signal using adaptive filter at 3m distance

(c) Reflected signal using exponential filter at 3m distance

Figure 6.6: Reflected signal from figure 6.1 with different MTI filters applied, and a human at 3m distance

signal. The signal of the person will be 7 range bins wide, with the centre range bin having the most power, added to 1 number. Noise strength will be the remaining signal strength of the MTI filtered data added to 1 number. The performance factor F will be calculated as follows with $D_{i,j}$ being the data at i range bin and j row, and M being the range bin with the peak power.

$$F = \frac{\sum_{j=0}^{\infty}\sum_{i=M-3}^{M+3} D_{i,j}}{\sum_{j=0}^{\infty}\sum_{i=0}^{\infty} D_{i,j} - \sum_{j=0}^{\infty}\sum_{i=M-3}^{M+3} D_{i,j}} \tag{6.1}$$

Using the particular data from figure 6.6, and equation 6.1 the performance factor is as follows:

MTI Filter	Performance factor
Average filter	0.5375
Adaptive filter	0.6695
Exponential filter	0.7341

Table 6.1: MTI filter comparison using the performance factor

The performance factor shows that the exponential although a bit more complicated is more suitable for the MTI filter. The extra noise from the radar will be filtered with a low-pass filter.

6.2. Lowpass filter

A lowpass filter will be implemented to filter out the frequencies above 2Hz as the normal breathing rate will not go beyond 1 Hz for babies. But for the current setup, we have chosen to not include this lowpass filter as there is minor or diminishing effect on the performance.

6.3. Human Detection

Human detection is an important part of the three step algorithm. Why would one even attempt to measure someone vital signs if there is no person in the room? So to make sure that the radar is active at the right moments and not wasting energy and time, a human detection algorithm is implemented. For the human detection the experimental data of each person and that of the empty room is used. The idea is to compare the power of the data with a threshold value for each distance (1-5 m). The threshold value is found by looking at the lowest power for every meter between the two test subjects Haobo and Jiaqian and then halving this power. A curve is then made between these values.

Of course this threshold is only applicable to the experimental data and the location specific to where this data was obtained. Ideally the creation of the threshold values would be done during the set-up of the radar, by taking a few initial measurements of both your empty car and measurement with your child in the car.

6.4. range bin-decisions

While it is possible to use the algorithms discussed in the next chapter on the whole matrix of data, this is not only inefficient, but also redundant. As was shown in figure 3.2.B, Only a single line is needed to compare the differences of each received pulse and subsequently recover the frequency information of the object causing

Distance	Threshold value
1 m	0.0034
2 m	$9.5 \cdot 10^{-4}$
3 m	$3.05 \cdot 10^{-4}$
4 m	$1.85 \cdot 10^{-4}$
5 m	$1.15 \cdot 10^{-4}$

Table 6.2: Threshold values used for extrapolation

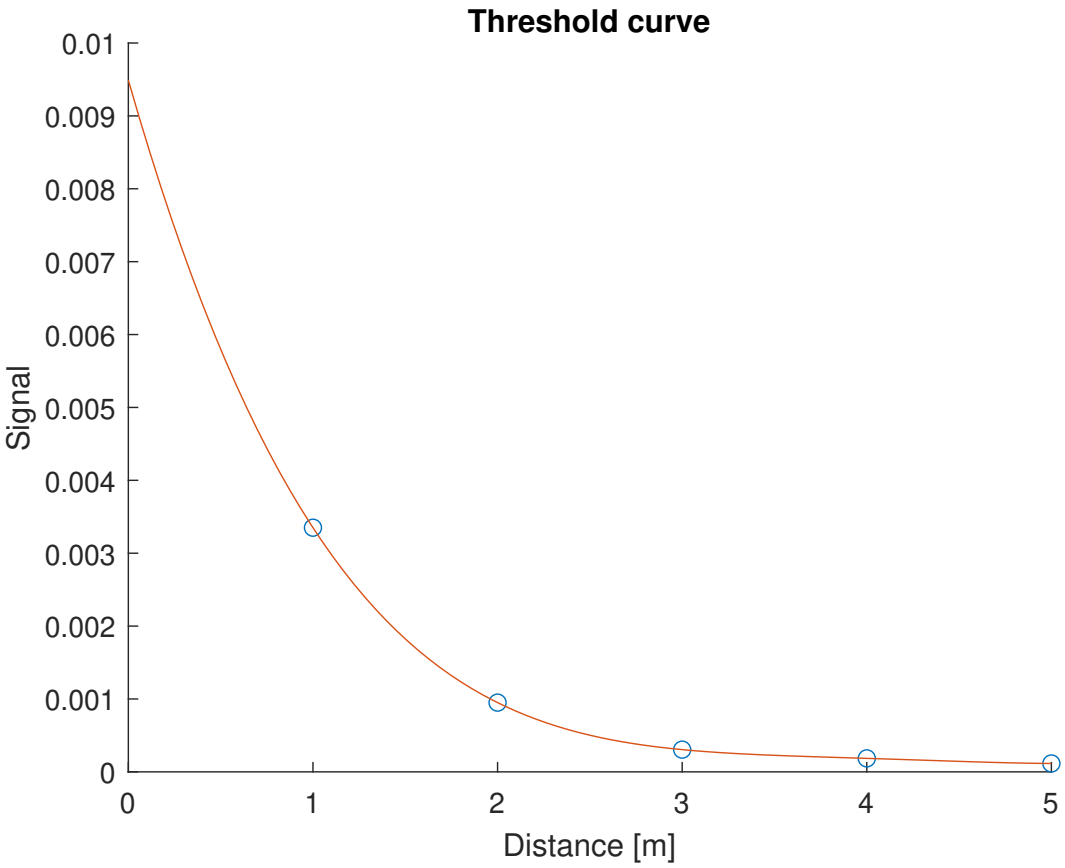

Figure 6.7: Threshold values extrapolated to 4th degree curve

the reflections. While putting this line on a spot where every single received pulse is 0 (the beginning or the end of the signal) would still give incorrect results, there is a range of options as to where one could "draw this line". In the algorithm the equivalent to drawing a line is taking a single range bin out of the range-time matrix. Since there are multiple range bins to choose from, different algorithms were designed for this and compared to each other. The algorithms that were created were named:

1. The summation of all the range bins in fast-time into a single range bin.
2. Using the range bin containing the most power.
3. Looking for the range bin that contains the peak signal.
4. Summing all the range bins that is higher than 1/4 peak signal.
5. Calculate the centre distance of the signal.
6. Using the cumulative sum on each range bin, and then add the range bins up.

To test these algorithms, a second performance factor was thought up and implemented in MATLAB. This factor compares the area under the wanted frequency components to that of the whole signal in frequency domain. The closer this factor is to 1 the better it is. To find the peaks belonging to the breathing frequencies all frequency components lower than 0.2 Hz are first removed since breathing can never be that low. Then by using the find peaks function with the correct parameters (code can be found in the appendix A.1)

for the integration we make use of the numerical trapezoid method.

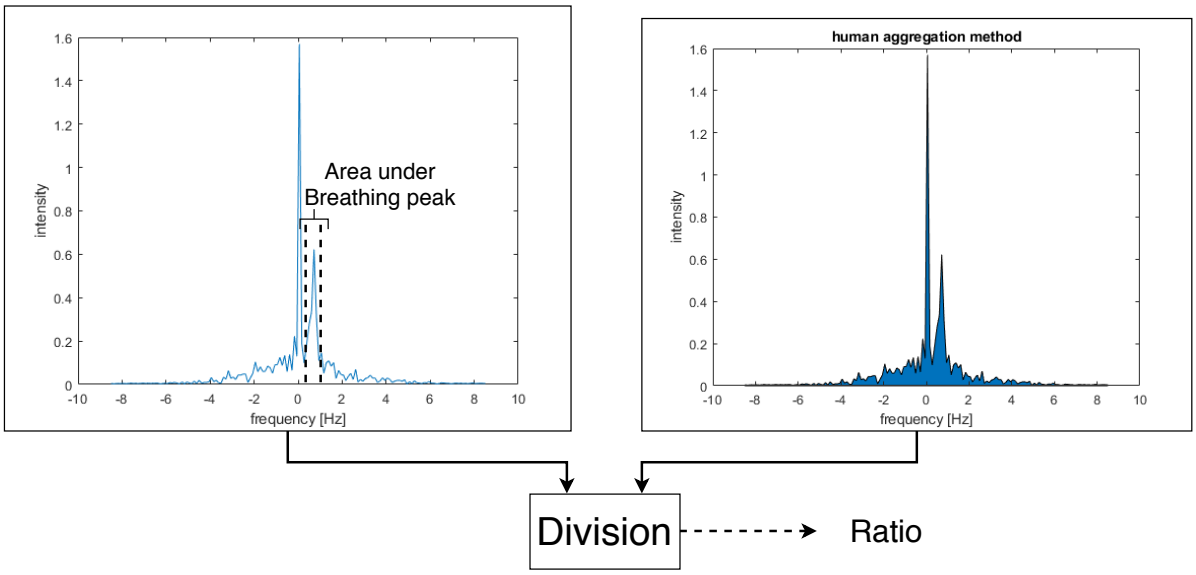

Figure 6.8: Calculation of performance factor range bin decisions

Peak locations of various data (Hz)	**2 meter**	**3 meter**
Sum all range bins	0.7222	0.6839
Highest summed value	0.7222	0.2931
Highest value	0.7222	0.2931
Human aggregation	0.7222	0.6839
Bad range bin (index 44/17)	0.2007	0.2008

Table 6.3: Location of the peaks of the fft signal of experimental data from a person at 2 meters and at 3 meters away. Not filtered

Table 6.3 shows that some of the peak locations are different from others. This is because in the unfiltered data of 3 meters there is a huge dc component in the matrix which would thus make methods 2&3 pick that range bin instead of one where the frequency can be found inside of. Filtering the signal however gives the new table:

Peak locations of various data (Hz)	**2 meter**	**3 meter**
Sum all range bins	0.7222	0.6839
Highest summed value	0.7222	0.7816
Highest value	0.7222	0.7816
Human aggregation	0.7222	1.5632
Bad range bin (index 44/17)	0.2007	-3

Table 6.4: Location of the peaks of the fft signal of experimental data from a person at 2 meters and at 3 meters away. Filtered

It shows that after filtering the second and third row of the table get more realistic values, although they still differ with 0.1 Hz from the summation method. The human aggregation method, however starts to falter. However upon human inspection of the frequency spectrum it was found that there exist two high peaks in the frequency spectrum. With the highest at around 1.5 Hz and the one slightly beneath that located at 0.68 Hz (figure 6.9). Finally the last two tables show the calculated ratio's for the filtered and unfiltered data:

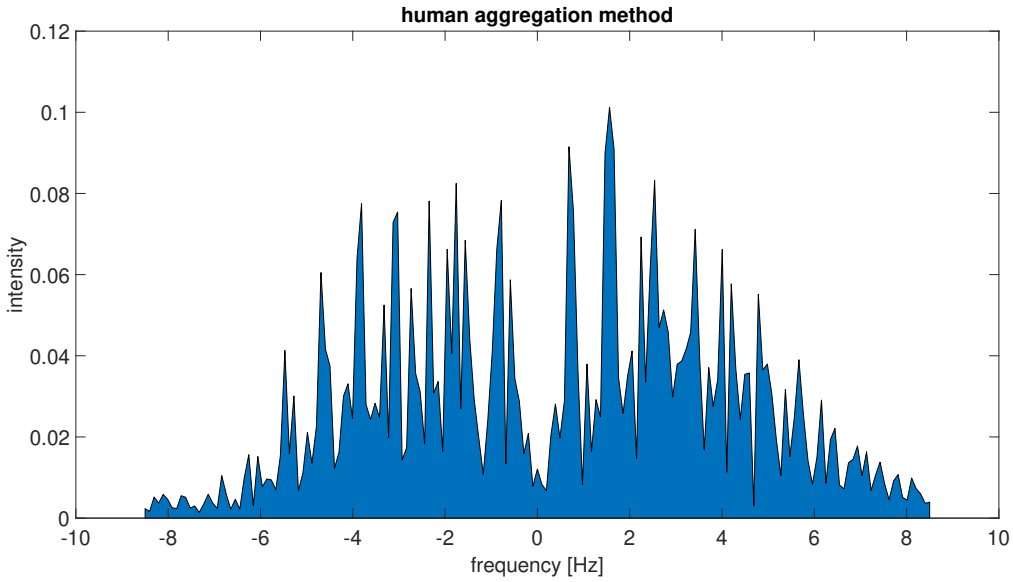

Figure 6.9: Peaks of human aggregation method

Ratio	**2 meter**	**3 meter**
Sum all range bins	0.33866	0.1287
Highest summed value	0.1910	0.0081
Highest value	0.1910	0.0081
Human aggregation	0.2201	0.1118
Bad range bin	0.1912	0.1095

Table 6.5: Ratio between area under the peak and area under the rest of the graph. Not filtered

Ratio	**2 meter**	**3 meter**
Sum all range bins	0.2512	0.1153
Highest summed value	0.1886	0.1451
Highest value	0.1886	0.1451
Human aggregation	0.3178	0.1139
Bad range bin	0.2026	0.1318

Table 6.6: Ratio between area under the peak and area under the rest of the graph. filtered

So for two meters all methods are just as accurate, but summation and aggregation have the highest power under the breathing frequency peak. However for 3 meters method 4 is inaccurate and methods 2&3 reach here the highest ratio. All in all methods 2/3 and the summation of all range bins are the best since accuracy is the most important factor.

7

Breathing Algorithm

After the MTI filter is is now possible to focus on the human part of the signal and determining the breathing rate. The breathing algorithm will be a comparison between four algorithms, for which two of them are well known in the literature.

7.1. Hilbert Huang transform

The Hilbert Huang transform is a signal processing technique that combines the empirical mode decomposition (EMD) with the Hilbert spectral analysis (HSA) [[20]]. The EMD process splits up signal into orthogonal basis intrinsic mode functions (IMF). An IMF is defined as a function that satisfies the following requirements:

- In the whole data set, the number of extrema and the number of zero-crossings must either be equal or differ at most by one.

- At any point, the mean value of the envelope defined by the local maxima and the envelope defined by the local minima is zero. [[21]]

The Hilbert Huang transform then uses these functions to create a time-frequency plot. So in addition to information about the frequency spectrum, the hht also displays how this spectrum changes with time (if it changes at all). Additionally the first IMF contains high frequency components(often noise) can be rejected by simply omitting it from the hht. The way EMD construct the IMF's is shown in figure 7.1. The advantages of the EMD is that it works on non-stationary and non-linear data. In MATLAB the transform is done by first calling the EMD() function and obtaining the IMF's belonging to the signal given to the function as a parameters. Then by putting these IMF's in the hht() functions. Much like the fft the hht also uses one of the columns from the Range-Time matrix to find the vital signs. To test if the algorithm works correctly the synthetic data from chapter 5 is used with frequencies 0.5 and 1.5. First the hht is done on just the distance vector itself, then on a column from the self-made pulse matrix using the highest value method and one using the summation of columns method. as shown in figure 5.5a the RTI matrix has a nearly dc component at 2 meters, which makes it hard to extract the frequency information from these columns, so to bypass this issue, an offset of 300 indices is given to the maximum value method. All three of the graphs show frequency components and 0.5 and 1.5, With the only inaccuracies happening at the beginning and the end of the graph. Also since there are only two frequency components in the synthetic data, removing the first imf wouldn't result in the removal of noise but in the removal of the highest frequency component (1.5 Hz). So for this figure the first imf was included.

The only downsize to the Hilbert Huang transform is that its a very sophisticated technique. This means that it hasn't been used in many different application and thus the hardware isn't as widely used as some of the other techniques discussed in this paper. While there is work being done on making the hardware implementation of the Hilbert Huang transform as efficient as possible [[22], [23]], for our radar implementation fast processing of the data is a must.

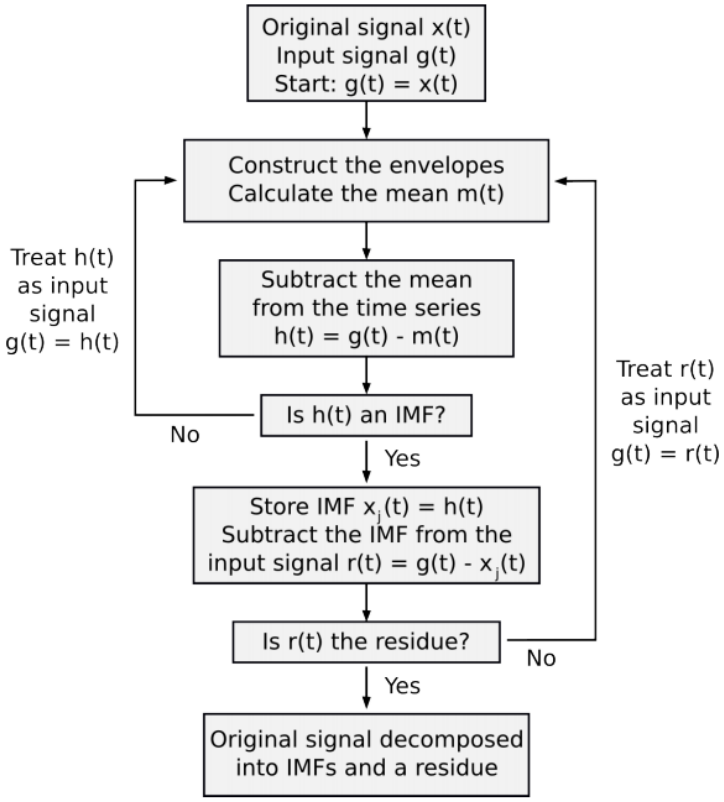

Figure 7.1: Block diagram of Empirical mode decomposition [21]

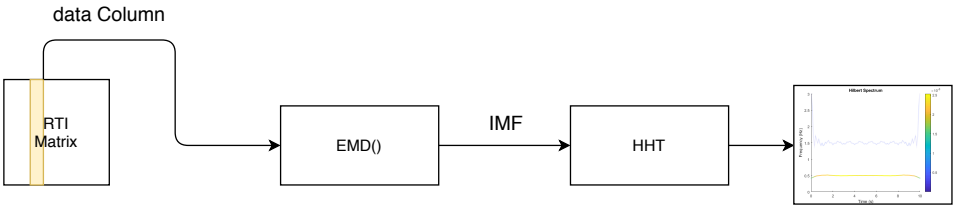

Figure 7.2: Block diagram of Hilbert Huang transform implementation

7.2. Fast Fourier transform

The Fourier transform is defined as:

$$F(\omega) = \int_{-\infty}^{\infty} f(t) * e^{-j\omega t} dt \tag{7.1}$$

This transform results in the frequency spectrum of a function f(t). The digital implementation of the Fourier transform is called the DFT (discrete Fourier transform) which calculates the Fourier transform using discrete samples of the signal. The complexity of the DFT is $\mathcal{O}(n^2)$. The fft is an improvement on the DFT and decreases the complexity to just $\mathcal{O}(n \log n)$. The fft is the most commonly used algorithm discussed in this thesis both in hardware and software.

In MATLAB the fft can be obtained by simply calling the fft() function. To plot the fft we also shift the spectrum so that the plot shows both the positive and negative frequency. Also the frequency axis, called the Doppler axis in the code, is created by creating a vector with values between the bandwidth of the signal (-PRF/2 PRF/2). Similar to the hht transform two plots using two of the column detection methods will be plotted to showcase the correctness of this algorithm. Note however that for these plots the synthetic filter was first put through the exponential filter, with the effect that the very strong dc component (originating from $d0$) is subdued: Comparing figure 7.4 with figure 5.3 indeed shows that the vital information can be obtained using the fast fourier transform.

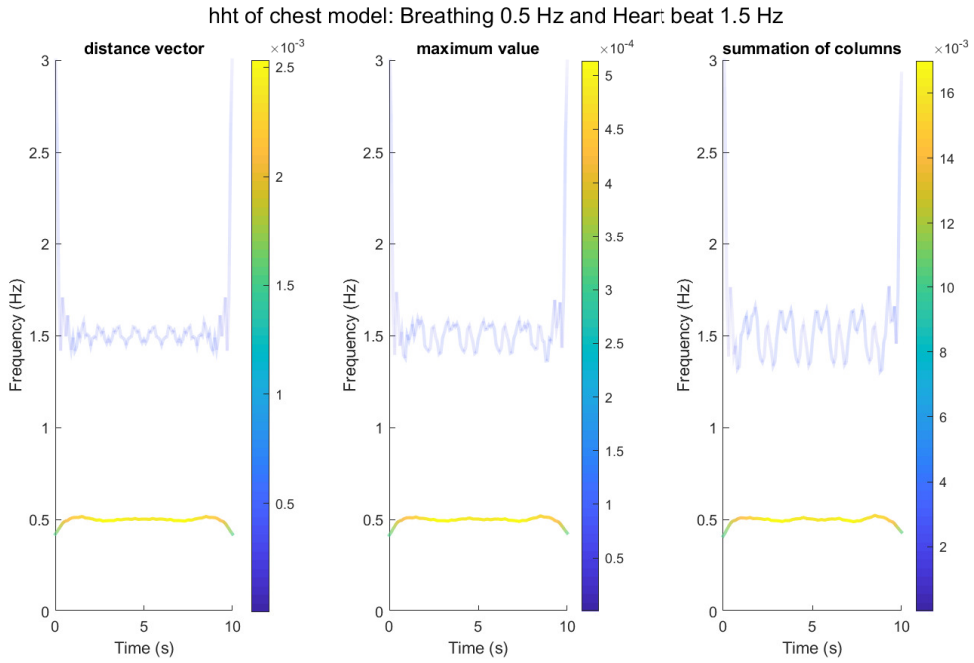

Figure 7.3: Hht both on distance vector and on pulse matrix of synthetic data

7.3. Centroid

The centroid method relies on the range variations in the measurements data. This algorithm calculates the centroid of each fast-time signal and assumes that the only varying object in the radar would be the chest movement. This algorithm can also be seen as the expected value of the signal if the signal is treated as a probability distribution. From this we can conclude that the expected value of the noise contribution is 0. This method eliminates the need of a filter, but will need an average value to move the centroid signal down to the x-axis. The centroid algorithm is also highly sensitive to other moving objects that is independent of the chest.

In figure 7.5 are the output data of the centroid algorithm along with the fft of that signal. The output signal is in line with figure 5.2a, but with some added noise caused by the re-sampling.

7.4. Cumulative sum (CumSum)

As the MTI filter is based on the exponential MTI filter, we can also treat it as a differentiation of the signal. This is because the moving average tracks the previous signals, subtracting it would create a illusion of differentiation. The outcome of the low-pass filter is then a smoothed differentiation like signal. To recreate the original chest expansion, the cumulative sum is used to integrate towards the slow-time axis (figure 7.6a) and then added together (figure 7.6b).

Comparing figure 7.6b with figure 5.2a we can see that the signal produced by the CumSum has a heart rate of a larger magnitude. This results in a significantly higher peak (figure 7.6c) towards the heart rate frequency at $1.2Hz$, the cause of this behaviour is currently unknown.

Out of these 4 algorithms we have tested the CumSum algorithm is best suited as the Hilbert Huang transform is a complex task in hardware, and

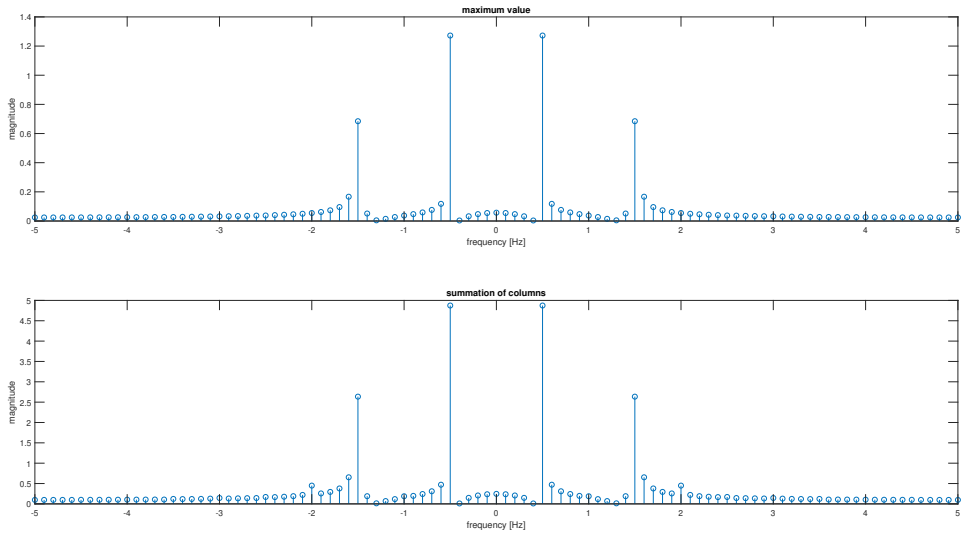

Figure 7.4: Fft on the pulse matrix of synthetic data

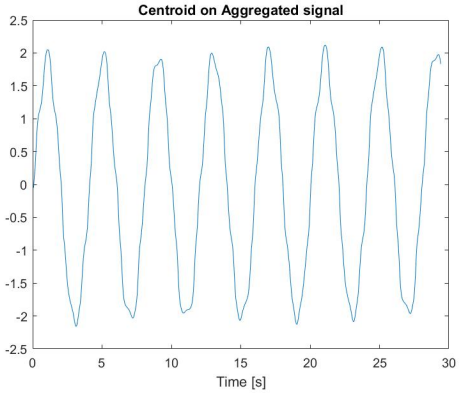

(a) Output of the centroid algorithm as a function of time and displacement

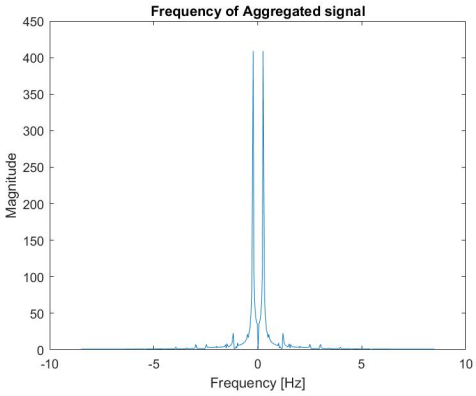

(b) Frequency composition of the centroid signal

Figure 7.5: Output of the centroid algorithm and a frequency composition of the output data

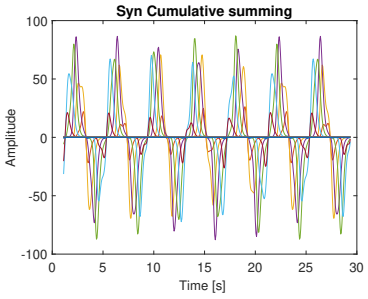

(a) Integrated signal of the exponential filtered data

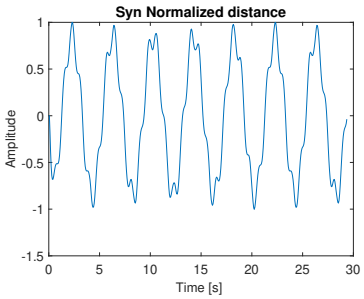

(b) The integrated signals added together as the output of the CumSum algorithm which implies the individual breaths

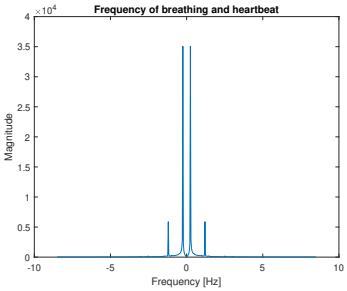

(c) Frequency composition of the CumSum signal

Figure 7.6: Different stages in the CumSum algorithm

8

Results

After verifying the algorithms with synthetic data, the algorithms will be tested using real world data. In this chapter the results of the algorithms are showcased with the experimental data from third party. The algorithms are tested on the experimental data of subject1, 24 years old male, Front data (figure 8.1b). This data does not have any variations in breathing rate or the amplitude and is most suitable to test a steady breathing. In the subject1 Front measurements he is seated 3 meters away from the radar, which is a lot further than a baby would sit from the radar in a car. So in addition to subject1 front, the last 10 seconds, when he breaths regularly, of subject 1 1m (figure 8.1a) are also tested. The algorithms will be tested with the data filtered by the exponential filter except for the hht algorithm where the first imf will be discarded instead.

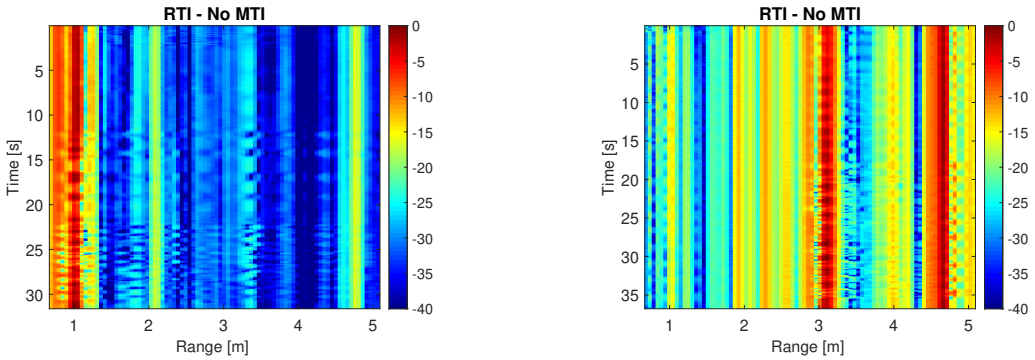

(a) subject1 1m experimental data

(b) subject1 Front experimental data

Figure 8.1: Experimental data used for the algorithms

8.1. Experimental results

8.1.1. Hht

The plots of the hilbert spectrum for the data at 1 and 2 meters are given by figure 8.2, figure 8.3 and finally using the subject1 front measurements in figure 8.4. As can be seen from the images the 1m sits around 1 the 2 meters around 0.7 and the front around 0.5 Hz breathing frequency.

8.1.2. CumSum

Using CumSum on the subject1 1m experimental data gives us a nice estimation (figure 8.5a) of what the individual breaths look like. In the last 10 seconds, figure 8.5b, he breathes regularly and deeply resulting in a displacement that is more noticeable, which gives a nice peak in the frequency plot at 1Hz (figure 8.5c). The heart rate is not distinguishable from other frequencies.

Applying CumSum on subject1 Front, figure 8.6, shows a clear breathing rate at 0.54Hz, figure 8.6c. Although we are not sure what the actual breathing rate is for subject1 at that specific moment, it is likely that

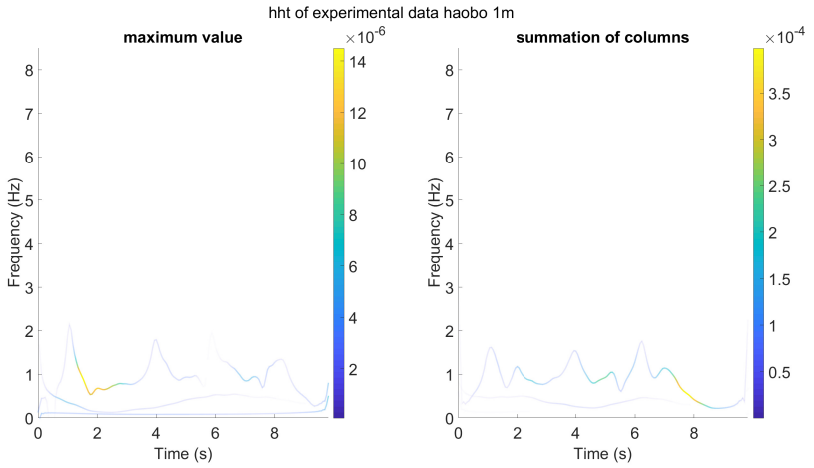

Figure 8.2: HHt on subject1 1m

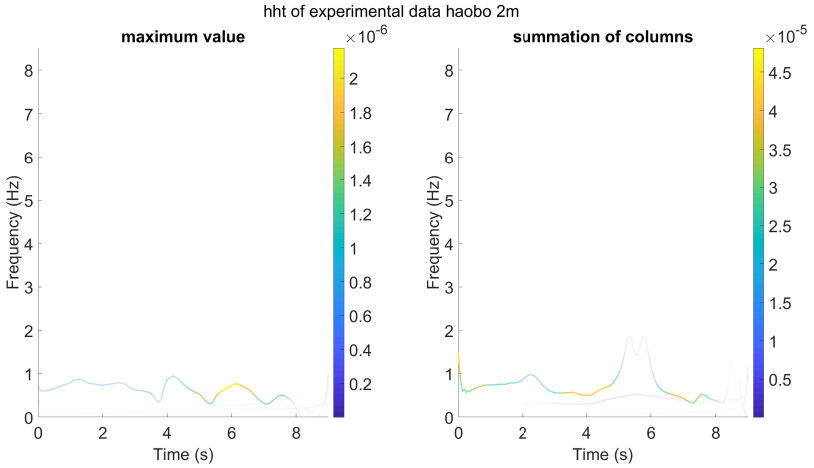

Figure 8.3: HHt on subject1 2m

his breathing rate is at 0.5Hz. For the heart rate it is unfortunately not possible to distinguish the frequency of the heart rate from other frequencies that are present.

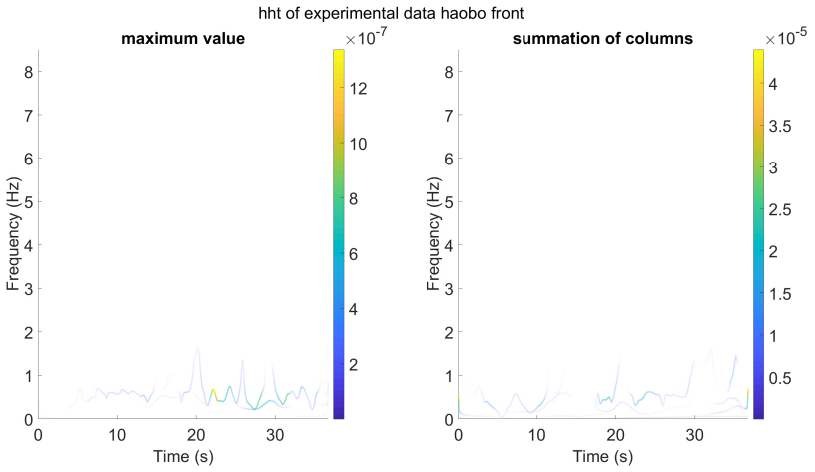

Figure 8.4: HHt on subject1 front

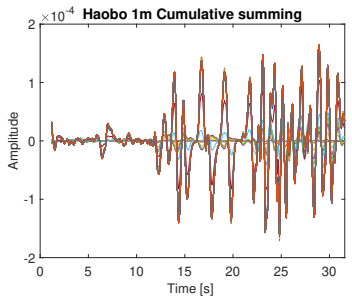

(a) The intermediate signal in the CumSum algorithm

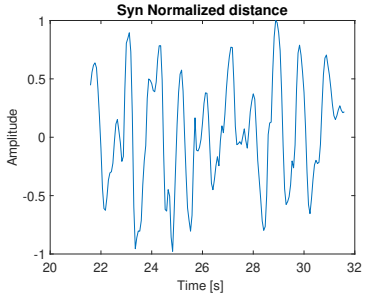

(b) Last 10 seconds after the CumSum algorithm with the amplitude of the distance displacement normalised

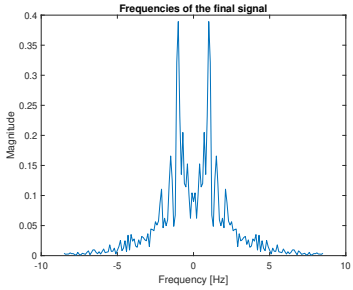

(c) Frequency plot of the final 10 seconds of subject1 1m with a peak at 1Hz

Figure 8.5: Graphs on experimental data subject1 1m

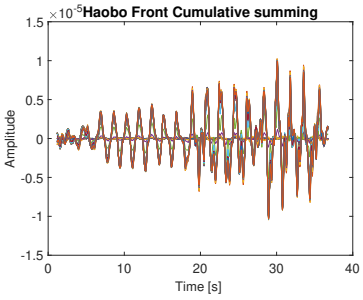

(a) The intermediate signal in the CumSum algorithm

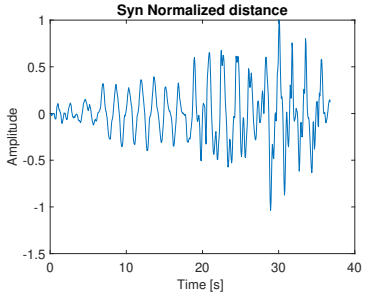

(b) Output signal using the CumSum algorithm with the amplitude of the distance displacement normalised

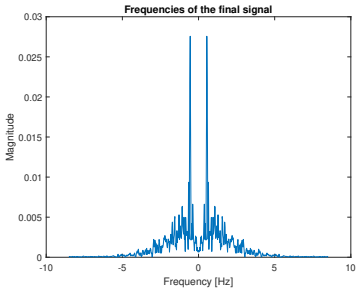

(c) Frequency plot of subject1 Front with a peak at 0.54Hz

Figure 8.6: Graphs on experimental data subject1 Front

9

Conclusion and Recommendations

9.1. Conclusion

Assuming that the displacement detected by the radar is caused by the breathing of the human, it is possible to extract the chest movements to determine the breathing rate. The following assumptions are made:

- Breathing causes chest movement
- Chest movement is the only moving object in the vicinity
- The movement of the chest can be described as a sinusoidal wave

Using a cumulative summing towards an exponential MTI filter acts as a integrator after a differentiation which reconstructs the original signal without the clutters that is observed by the radar. This method also removes the noise by having a low pass filter after the MTI filter. The processing scheme would be the following:

1. MTI filter (differentiation)
2. Low-pass filter (noise removal)
3. Cumulative summing (integrator)
4. Signal addition (data simplification)

9.2. Recommendation

For future research it is recommended to have a ground truth for what the breathing rate is. This can be achieved by telling the test subject to breath with a specific breathing rate or using a other detecting systems without obstructing the chest movement. The chest movement due to heart rate might be less clear because the human is also wearing clothes which minimises the visibility towards the small chest movement. It is noted that the heart rate is more difficult or not possible to detect using the radar at such low distance accuracy. For XeThru the radar can be adjusted for a higher resolution at a specific distance, which the experimental data does not have.

It would also be a nice addition to look towards implementation in a single chip, without using a dedicated fft chip to opt for extracting the frequency of the breathing rate, but looking at the time between the peaks which translates to the breathing rate.

A further research on how the lowpass filter would have affected the whole circuit in the real life case is also interesting approach to if the filter is necessary.

A

matlab code

A.1. SNRfreq function

Function to calculate ratio between area under peak and area under graph. also determines breathing rate peak.

```
%test viability of algorithm by looking at area under "wanted" peak and the
%rest
function [ratio,peak_location] = SNR_freq(signal, doppleraxis)
%remove dc frequency
    signal=abs(signal);
    total_area=trapz(doppleraxis,signal)
    right_bound=find(-0.2<doppleraxis & doppleraxis<0.2);
    signal(right_bound(1):right_bound(end))=0;
    [value_max,index_max]= max(signal)
    [pks,locs,width] = findpeaks(signal,doppleraxis,'MinPeakDistance',0.5,...
    'SortStr','descend','NPeaks',4)
    peak_area=pks(1)*width(1)+pks(2)*width(2)
    ratio=peak_area/total_area
    peak_location=locs(1)
end
```

A.2. chest model function

Function to set up matlab model of chest movement.

```
function [time_delay, chest_exp] = chest_model(breath_rate, heart_rate, time,d0,breath_ampl,heart

    f_b=breath_rate;
    f_h=heart_rate;
    Distance=d0+breath_ampl*sin(2*pi*f_b*time) +  heart_ampl*sin(2*pi*f_h*time);
    time_delay=2*Distance/physconst('LightSpeed');
    chest_exp=Distance;
end
```

A.3. chest model testing

This code tests the chest model and creates Range-Time matrix from it.

```
close all;
clear all;
PRF=10;
slow_time=[0:1/PRF:10];
```

```
RangeAxis=[0:1/1000:5];
fast_time=2*RangeAxis/physconst('LightSpeed');
f_b=0.5;
f_h=1.5;
d0=2;
t0=2*d0/physconst('Lightspeed');
[t_delay, distance]=chest_model(f_b,f_h,slow_time,d0,0.05,0.02);
DopplerAxis=linspace(-PRF/2,PRF/2,size(distance,2));
freq_dis=fftshift(fft(distance));
figure
stem(DopplerAxis,abs(freq_dis))
title("frequency spectrum of distance from chest model")
xlabel('frequency [Hz]')
ylabel('magnitude')
ylim([0,3])


%
figure
imf=emd(abs(distance));
hht(imf(:,1:end),PRF,'FrequencyLimits',[0 3]);
title('distance vector')
%
figure
plot(slow_time,t_delay)

pulse_range(:,:) = normpdf(RangeAxis,distance',0.6);


for i=1:20
    hold on
    txt = ['pulse ',num2str(i)];
    plot(RangeAxis,pulse_range(i,:),'DisplayName',txt)

end
title('Periodic movement of pulses')
ylabel('magnitude')
xlabel('range [m]')
legend
%% filter
Data_data=pulse_range;

Data_RTI_MTIExp(length(slow_time),length(RangeAxis))=0;

old_data=Data_data(1,:);
av_data1=pulse_range(1,:);
for i=1:length(slow_time)
    av_data1=0.7*av_data1+0.3*old_data;
    Data_RTI_MTIExp(i,:)=Data_data(i,:)-(av_data1);

    old_data=Data_data(i,:);
end
figure;
imagesc(RangeAxis,slow_time,20*log10(abs(Data_RTI_MTIExp./max(Data_RTI_MTIExp(:)))))
colormap('jet'); set(gca,'FontSize',14); title('RTI - MTI with Exponential')
xlabel('Range [m] ','FontSize',14); ylabel('Time [s]','FontSize',14);caxis([-40 0]);colorbar;
```

```
figure
imagesc(RangeAxis,slow_time,20*log10(abs(pulse_range./max(pulse_range(:)))))
colormap('jet'); set(gca,'FontSize',14); title('RTI synthetic data')
xlabel('Range [m] ','FontSize',14); ylabel('Time [s]','FontSize',14);caxis([-40 0]);colorbar;

%% column decisions
%find column with highest value
%Data=Data_RTI_MTIExp;
Data=pulse_range;
DopplerAxis=linspace(-PRF/2,PRF/2,size(Data,1));
maxValue = max(abs(Data), [], 'all');
[rowsOfMaxes, colsOfMaxes] = find(abs(Data) == maxValue);
%fft
freq=fftshift(fft(Data(:,colsOfMaxes(1)  )));
figure
subplot(2,1,1)
stem(DopplerAxis,abs(freq))
title('maximum value')
ylabel("magnitude")
xlabel("frequency [Hz]")
%sum of all columns
m=0;
m = sum(Data,2);
%ftt
freq=fftshift(fft(m));
subplot(2,1,2)
stem(DopplerAxis,abs(freq))
title('summation of columns')
ylabel("magnitude")
xlabel("frequency [Hz]")
%% centroid
Aggregated_signal = abs(Data)*RangeAxis';
Aggregated_signal=detrend(Aggregated_signal);
DopplerAxis2=linspace(-PRF/2,PRF/2,size(Aggregated_signal,1));
freq=fftshift(fft(Aggregated_signal));
figure
stem(DopplerAxis2,abs(freq))
title('centroid')


%% hilbert huang
figure
subplot(1,3,1)
imf=emd(abs(distance));
hht(imf(:,1:end),PRF,'FrequencyLimits',[0 3]);
title('distance vector')
subplot(1,3,2)
imf=emd(abs(Data(:,colsOfMaxes(1)+300  )));
hht(imf(:,1:end),PRF,'FrequencyLimits',[0 3]);
title('maximum value')
subplot(1,3,3)
imf=emd(abs(m));
hht(imf(:,1:end),PRF,'FrequencyLimits',[0 3]);
title('summation of columns')
```

```
sgtitle('hht of chest model: Breathing 0.5 Hz and Heart beat 1.5 Hz')
```

B

CumSum Algorithm

```
%% SynData test
clear all
close all
clc

%% Experimental data
dir='C:\Users\hans5\Desktop\Data 27062018\';
% file=strcat(dir,'haobo 1m\xethru_baseband_ap_20180627_150235.dat');
file=strcat(dir,'haobo front\xethru_baseband_ap_20180713_155037.dat');
% file=strcat(dir,'empty\xethru_baseband_ap_20180817_171535.dat');

[hdrMat , FrameMat] = ReadBasebandFile_new_version( file );
[numFrames, numHdrs] = size(hdrMat);
hdr = hdrMat(1,:);
BinLength = hdr(3); % in [m]
StartRange = hdr(6); %in [m]
FrameLength = hdrMat(1,2);

Data_intensity=FrameMat(1:size(FrameMat,1)/2,:);
Data_intensity=Data_intensity';
Data_phase=FrameMat(size(FrameMat,1)/2+1:size(FrameMat,1),:);
Data_phase=Data_phase';
Data_RTI_complex=sqrt(Data_intensity).*exp(1i*Data_phase);

PRF=17;
RangeAxis=StartRange+BinLength*(0:size(Data_intensity,2)-1);
TimeAxis=[1:size(Data_intensity,1)]/PRF;

figure
imagesc(RangeAxis,TimeAxis,20*log10(abs(Data_RTI_complex./max(Data_RTI_complex(:)))))
colormap('jet'); set(gca,'FontSize',14); title('RTI - No MTI')
xlabel('Range [m] ','FontSize',14); ylabel('Time [s]','FontSize',14);caxis([-40 0]);colorbar;

Syn=Data_intensity;

%% Synthetic Data

% numFrames=500;
% FrameLength=50;
% BinLength = 0.2;    %[m]
```

```
% StartRange = 0.9;   %[m]
% PRF=17;
% RangeAxis=StartRange+(0:FrameLength-1)/FrameLength*BinLength;
% TimeAxis=(0:numFrames-1)/PRF;
%
% BreathingRate=0.25;
% HeartRate=1.2;
% D0=1;
% Db=0.008*sin(BreathingRate*TimeAxis*2*pi);
% Dh=0.0005*sin(HeartRate*TimeAxis*2*pi);
% Dt=D0+Db+Dh;
% Dt=Dt';
%
% figure;
% plot(TimeAxis, Dt);
%
% DopplerAxis=linspace(-PRF/2,PRF/2,size(Dt,1));
% Dt_fft=fftshift(fft(Dt-D0),1);
%
% figure
% plot(DopplerAxis, abs(Dt_fft));
% title('Frequency of breathing and heartbeat')
% xlabel('Frequency [Hz]')
% ylabel('Magnitude')
%
% PulseWidth=16/1.5e3;
% % PulseWidth=0.06;
% Syn(:,:)=normpdf(RangeAxis,Dt,PulseWidth/4);
% % Syn(:,:) = awgn(Syn,1);
%
% figure;
% % subplot(2,4,1);
% imagesc(RangeAxis,TimeAxis,20*log10(abs(Syn./max(Syn(:)))))
% colormap('jet'); set(gca,'FontSize',14); title('Syn RTI')
% xlabel('Range [m] ','FontSize',14); ylabel('Time [s]','FontSize',14);caxis([-40 0]);colorbar;
%
% % figure
% % plot(RangeAxis, Syn);
% % set(gca,'FontSize',14);
% % title('Syn Range signal');
% % xlabel('Range [m] ','FontSize',14);
% % ylabel('Signal','FontSize',14);

%% Exp
Data_data=Syn;
av_data=Syn(1,:);
old_data=Syn(1,:);
for i=1:numFrames
    av_data=0.7*av_data+0.3*old_data;
    Data_RTI_MTIExp(i,:)=Data_data(i,:)-(av_data);

    old_data=Data_data(i,:);
end

figure;
imagesc(RangeAxis,TimeAxis,-sign(real(Data_RTI_MTIExp))*20.*log10(abs(Data_RTI_MTIExp./max(Data_RTI_MTI
```

```
colormap('jet'); set(gca,'FontSize',14); title('Syn MTI Exp 0.7')
xlabel('Range [m] ','FontSize',14); ylabel('Time [s]','FontSize',14);caxis([-40 40]);colorbar;


%% LowPass
Data_data=Data_RTI_MTIExp;
av_data=Data_RTI_MTIExp(1,:);
old_data=Data_RTI_MTIExp(1,:);
for i=1:numFrames
    av_data=0.5*av_data+0.5*old_data;
    old_data=Data_data(i,:);
    Data_RTI_MTILow(i,:)=(av_data);
end

figure;
imagesc(RangeAxis,TimeAxis,-sign(real(Data_RTI_MTIExp))*20.*log10(abs(Data_RTI_MTILow./max(Data_R
colormap('jet'); set(gca,'FontSize',14); title('Syn MTI Lowpass0.5')
xlabel('Range [m] ','FontSize',14); ylabel('Time [s]','FontSize',14);caxis([-40 40]);colorbar;

figure
plot(RangeAxis, Data_RTI_MTILow);
set(gca,'FontSize',14);
title('Computed Syn Range-difference signal');
xlabel('Range [m] ','FontSize',14);
ylabel('Intensity','FontSize',14);

%% Cumulative sum Sum
Data_Sum=cumsum(Data_RTI_MTILow,2);

figure
plot(TimeAxis(20:end), Data_Sum(20:end,:));
set(gca,'FontSize',14);
title('Haobo Front Cumulative summing')
xlabel('Time [s] ','FontSize',14);
ylabel('Amplitude','FontSize',14);

%% Distance signal

% S=numFrames-170;
% S=1;

Data_Distance=sum(Data_Sum(S:end,:),2);

figure
plot(TimeAxis(S:end), Data_Distance/max(Data_Distance));
set(gca,'FontSize',14);
title('Haobo Front Normalized distance')
xlabel('Range [m] ','FontSize',14);
ylabel('Amplitude','FontSize',14);


%% Fourier
DopplerAxis=linspace(-PRF/2,PRF/2,size(Data_Distance,1));
Data_Distance_fft=fftshift(fft(Data_Distance),1);

figure
```

```
plot(DopplerAxis, abs(Data_Distance_fft));
title('Frequencies of the final signal')
xlabel('Frequency [Hz]')
ylabel('Magnitude')
```

C

Code for experimental data

C.1. Read baseband file

This code translates the Xethru baseband ".data" file from the Xethru radar chip to a range-time matrix that can be used in matlab.

```
function [ hdrMat, FrameMat ] = ReadBasebandFile_new_version( file )
%UNTITLED Summary of this function goes here
%   Detailed explanation goes here

NumHdrs = 6;

fid = fopen(file, 'rb');
if fid < 3
    disp(['couldnt read file ' file]);
    return
end

f = dir(file);
fsize = f.bytes;

% read first frame
ctr = 0;
hdrMat = [];
FrameMat = [];
TimeVec = [];

while (1)
    if feof(fid)
        break
    end

    % read header
    frameCtr = fread(fid, 1,'uint32');
    numBins = fread(fid, 1,'uint32');
    binLength = fread(fid, 1,'single');
    Fs = fread(fid, 1,'single');
    Fc = fread(fid, 1,'single');
    RangeOffset = fread(fid, 1, 'single');

    % check valid header read
    if isempty(frameCtr) || isempty(numBins) || isempty(binLength) || isempty(Fs) ...
```

```
            || isempty(Fc) || isempty(RangeOffset)
        break;
    end

    % read data
    data = fread(fid, 2*numBins, 'single');
    if ctr==0
       numFrames = fsize / (4*(NumHdrs + 2*numBins));
       hdrMat = zeros(numFrames, NumHdrs);
       FrameMat = zeros(2*numBins, numFrames);
    end
    ctr = ctr + 1;

    hdrMat(ctr,:) = [double(frameCtr) double(numBins) binLength Fs Fc RangeOffset];
    FrameMat(:,ctr) = data;

end

[n,m] = size(hdrMat);
disp([file ' read. NumFrames=' num2str(n)]);
fclose(fid);
```

Bibliography

[1] D. Orlando, C. Hao, A. Aubry, G. Cui, A. C. Gurbuz, and S. Gazor, "Special issue: Advanced techniques for radar signal processing", EURASIP Journal on Advances in Signal Processing, 2017. DOI: 10.1186/s13634-017-0481-0.

[2] M. Hines, There's science behind why parents leave kids in hot cars, Aug. 2019. [Online]. Available: https://eu.usatoday.com/story/news/health/2019/08/02/hot-car-deaths-why-they-keep-happening-and-how-stop-them/1861389001/.

[3] M. Richards, J. Scheer, J. Scheer, and W. Holm, Principles of Modern Radar: Basic Principles, Volume 1, ser. Electromagnetics and Radar. Institution of Engineering and Technology, 2010, ISBN: 9781891121524. [Online]. Available: https://books.google.nl/books?id=nD7tGAAACAAJ.

[4] C. Li, J. Cummings, J. Lam, E. Graves, and W. Wu, "Radar remote monitoring of vital signs", IEEE Microwave Magazine, vol. 10, no. 1, pp. 47–56, 2009.

[5] M. Kebe, R. Gadhafi, B. Mohammad, M. Sanduleanu, H. Saleh, and M. Al-qutayri, "Human vital signs detection methods and potential using radars: A review", Sensors (Switzerland), vol. 20, no. 5, 2020, ISSN: 14248220. DOI: 10.3390/s20051454.

[6] V. L. Petrović, M. M. Janković, A. V. Lupšić, V. R. Mihajlović, and J. S. Popović-Božović, "High-accuracy real-time monitoring of heart rate variability using 24 ghz continuous-wave doppler radar", IEEE Access, vol. 7, pp. 74 721–74 733, 2019.

[7] A. Rahman, E. Yavari, X. Gao, V. Lubecke, and O. Boric-Lubecke, "Signal processing techniques for vital sign monitoring using mobile short range doppler radar", 2015 IEEE Topical Conference on Biomedical Wireless Technologies, Networks, and Sensing Systems, BioWireleSS 2015, pp. 17–19, 2015. DOI: 10.1109/BIOWIRELESS.2015.7152126.

[8] H. Lee, B. H. Kim, J. K. Park, and J. G. Yook, "A novel vital-sign sensing algorithm for multiple subjects based on 24-GHz FMCW Doppler radar", Remote Sensing, vol. 11, no. 10, 2019, ISSN: 20724292. DOI: 10.3390/rs11101237.

[9] A. Lazaro, D. Girbau, and R. Villarino, "Analysis of vital signs monitoring using an IR-UWB radar", Progress in Electromagnetics Research, vol. 100, pp. 265–284, 2010, ISSN: 15598985. DOI: 10.2528/PIER09120302.

[10] A. Droitcour, V. Lubecke, J. Lin, and O. Boric-Lubecke, "A microwave radio for Doppler radar sensing of vital signs", IEEE MTT-S International Microwave Symposium Digest, vol. 3, pp. 175–178, 2001, ISSN: 0149645X. DOI: 10.1109/MWSYM.2001.966866.

[11] X. Liang, J. Deng, H. Zhang, and T. A. Gulliver, "Ultra-Wideband Impulse Radar Through-Wall Detection of Vital Signs", Scientic Reports, 2018. DOI: https://doi-org.tudelft.idm.oclc.org/10.1038/s41598-018-31669-y.

[12] L. Liu, Z. Liu, and B. E. Barrowes, "Through-Wall Bio-Radiolocation With UWB Impulse Radar: Observation, Simulation and Signal Extraction", IEEE Journal of Selected Topics in Applied Earth Observations and Remote Sensing, vol. 4, no. 4, pp. 791–798, 2011, ISSN: 21511535. DOI: 10.1109/JSTARS.2011.2157461.

[13] T. Covington, "Hot car death statistics in 2020", The Zebra, 2020. [Online]. Available: https://www.thezebra.com/research/hot-car-death-statistics/.

[14] FCC, "Radio frequency safety", FCC, 2019. [Online]. Available: https://www.fcc.gov/general/radio-frequency-safety-0.

[15] ICNIRP, “Guidelines for limiting exposure to electromagnetic fields (100khz to 300ghz)”, Health Physics, vol. 118, pp. 483–524, 2020. [Online]. Available: https://www.icnirp.org/cms/upload/publications/ICNIRPrfgdl2020.pdf.

[16] M. Mabrouk, S. Rajan, M. Bolic, I. Batkin, H. Dajani, and V. Groza, “Model of human breathing reflected signal received by pn-uwb radar”, 2014 36th Annual International Conference of the IEEE Engineering in Medicine and Biology Society, EMBC 2014, vol. 2014, pp. 4559–62, Aug. 2014. DOI: 10.1109/EMBC.2014.6944638.

[17] U. Karahasanovic, T. Stifter, H. Beise, A. Fox, and D. Tatarinov, “Mathematical modelling and simulations of complex breathing patterns detected by radar sensors”, in 2018 19th International Radar Symposium (IRS), Jun. 2018, pp. 1–10. DOI: 10.23919/IRS.2018.8448045.

[18] M. G. M. Hussain, “Ultra-wideband impulse radar-an overview of the principles”, IEEE Aerospace and Electronic Systems Magazine, vol. 13, no. 9, pp. 9–14, 1998.

[19] G. Shafiq and K. C. Veluvolu, “Surface chest motion decomposition for cardiovascular monitoring”, Scientific Reports, 2014. [Online]. Available: https://doi.org/10.1038/srep05093.

[20] N. Huang and Z. Wu, “A review on hilbert-hung transform method and its applications to geophysical studies”, Reviews of Geophysics, vol. 46, RG2006, Jun. 2008. DOI: 10.1029/2007RG000228.

[21] A. Zeiler, R. Faltermeier, I. Keck, A. Tomé, C. Puntonet, and E. Lang, “Empirical mode decomposition - an introduction”, Jul. 2010, pp. 1–8. DOI: 10.1109/IJCNN.2010.5596829.

[22] P. Chen, Y. Lai, and J. Zheng, “Hardware design and implementation for empirical mode decomposition”, IEEE Transactions on Industrial Electronics, vol. 63, no. 6, pp. 3686–3694, 2016.

[23] Li Hongsheng, Li Zhengqin, Chen Wenwu, and Zhao Zhao, “Implementation of hilbert-huang transform (hht) based on dsp”, in Proceedings 7th International Conference on Signal Processing, 2004. Proceedings. ICSP ’04. 2004., vol. 1, 2004, 499–502 vol.1.